Supporting Information:

Adsorptive removal of tetracycline and methylene blue from aqueous solution with a water resistance copper-based metal organic framework

Yingzhi Zhu,[a] Yan Li,[b] Na Ma,[b] and Wei Dai*,[a]

[a]*Key Laboratory of the Ministry of Education for Advanced Catalysis Materials, College of Chemistry and Materials Science, Zhejiang Normal University, Jinhua 321004, People's Republic of China*

[b]*College of Geography and Environmental Sciences, Zhejiang Normal University, Jinhua, 321004, PR China*

Corresponding author.

E-mail address: daiwei@zjnu.edu.cn (W. Dai)

Chemicals: Copper nitrate trihydrate ($Cu(NO_3)_2 \cdot 3H_2O$, 99 %) (Shanghai Aladdin Biotechnology Co., Ltd.); Tetracycline hydrochloride (98 %) (Beijing Bailingwei Technology Co., Ltd.); deionized water (generated at 25 ^oC, 18.25$m\Omega \cdot cm^{-1}$); Benzene-1,3,5-tricarboxylic acid (H_3BTC), sodium hydroxide (NaOH), hydrochloric acid (HCl), methylene blue (MB), Ethylene glycol ($(CH_2OH)_2$, AR) were purchased from Sinopharm Chemical Reagent Co., Ltd.

Apparatus: SEM images are scanned by electron microscope using Hitachi S4800 equipped with EDAX energy dispersion detector (Zeiss Gemini SEM 300). D8 Advance X-ray diffractometer of Bruck AXS GMBH is used to scan the crystal phase

of the material (2θ = 5~40°). The specific surface area and average pore diameter of the material are measured by Autosorb-iQ physical adsorption instrument of Kanta Instrument Co., Ltd. (The samples were degassed at 120 °C for 5h and The N_2 adsorption-desorption isotherms were recorded at -196 °C). The functional groups were analyzed by a Fourier transform infrared spectrometer (FT-IR, Thermo Nicolet NEXUS-670). And the sample absorbance was measured by Shimadzu UV-3600 spectrophotometer at 357 and 664 nm.

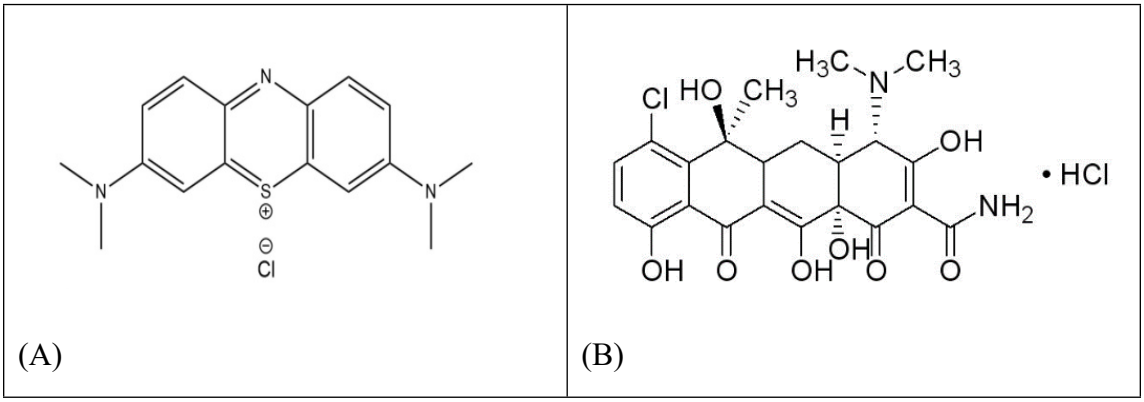

Scheme S1. The molecular formula of MB and TC

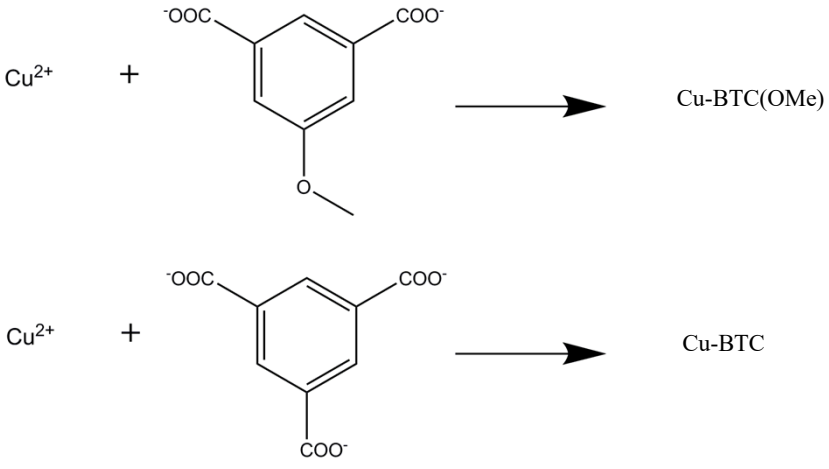

Scheme S2. Reaction diagrams of Cu-BTC(OMe), and Cu-BTC using a similar hydrothermal method.

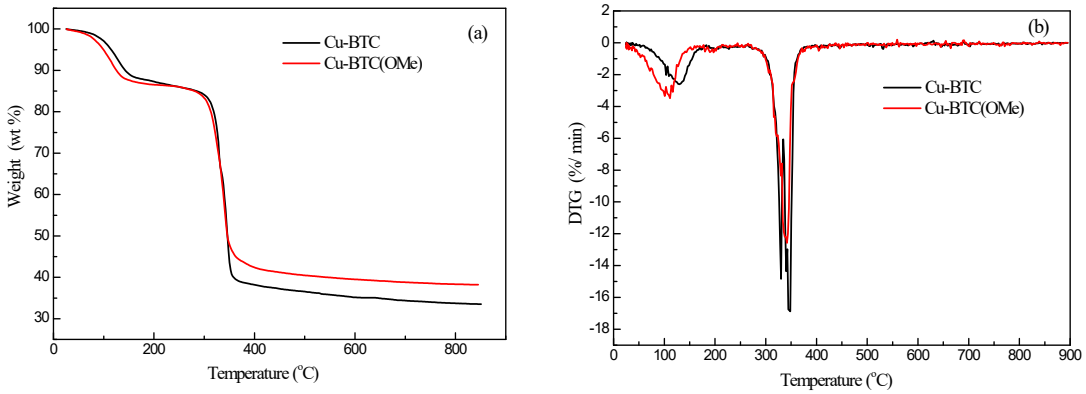

Fig. S1. Thermo-gravimetric curves of Cu-BTC and Cu-BTC(OMe): (a) TGA, (b) DTA.

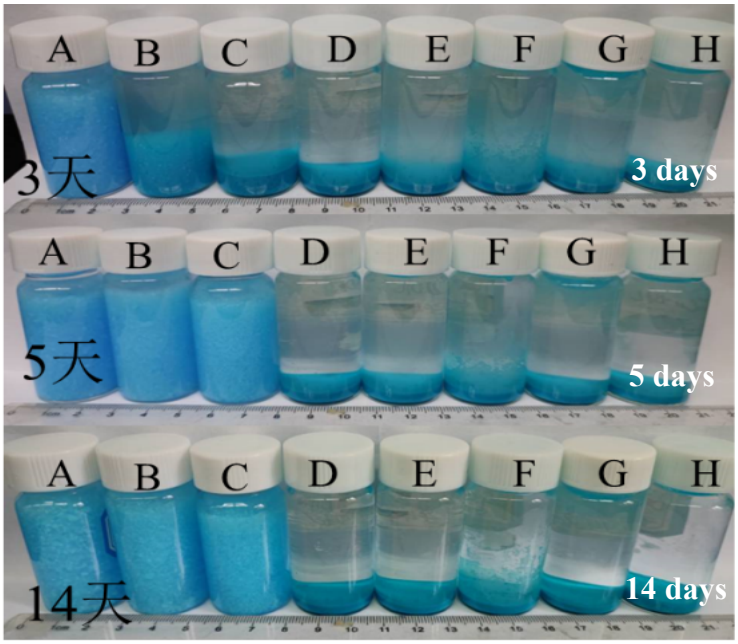

Fig. S2. The pictures of (A): Cu-BTC; (B): Cu-BTC(OMe5); (C): Cu-BTC(OMe10); (D): Cu-BTC(OMe15); (E): Cu-BTC(OMe20); (F): Cu-BTC(OMe30); (G): Cu-BTC(OMe40); and (H): Cu-BTC(OMe50) after soaking in water for 3, 5, and 14 days respectively.

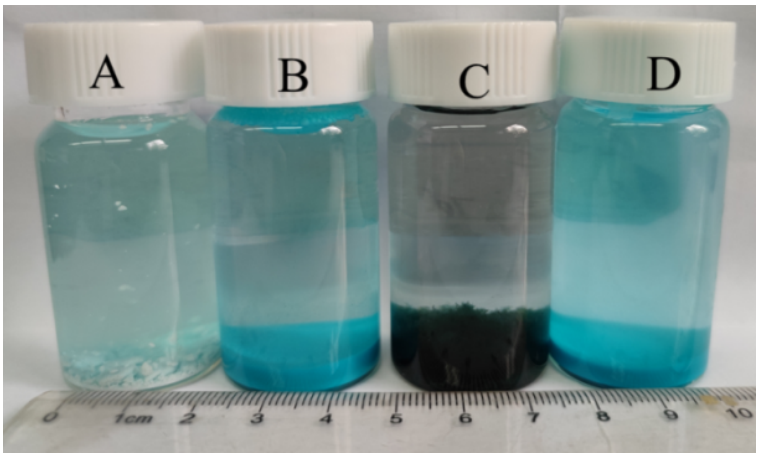

Fig. S3. The pictures of the Cu-BTC(OMe50) samples soaked in water at (A): pH=2; (B): pH=7; (C): pH=14 and (D): T=100 °C for 30 min.

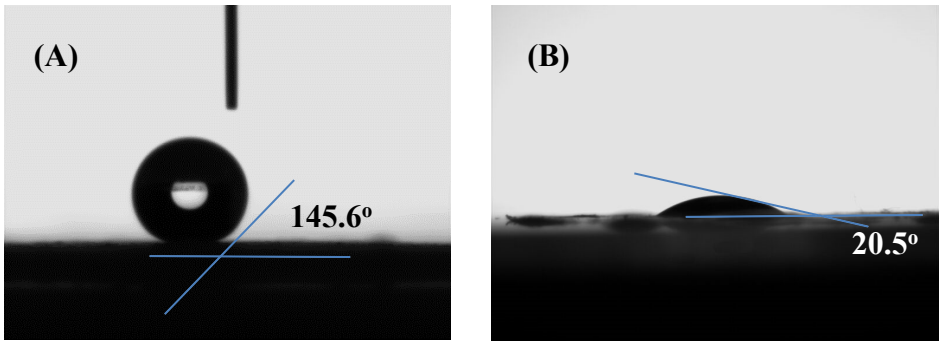

Fig. S4. Water contact angles of the (A): Cu-BTC(OMe50) and (B): Cu-BTC.

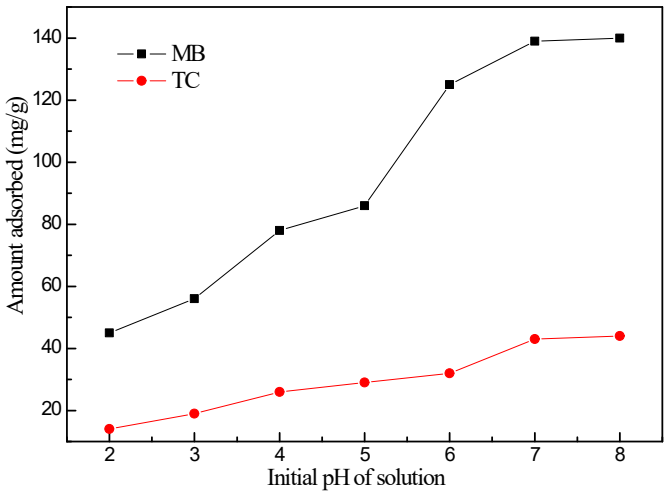

Fig. S5. Effect of solution pH on adsorption amounts of the MB and TC over Cu-

BTC(OMe50).

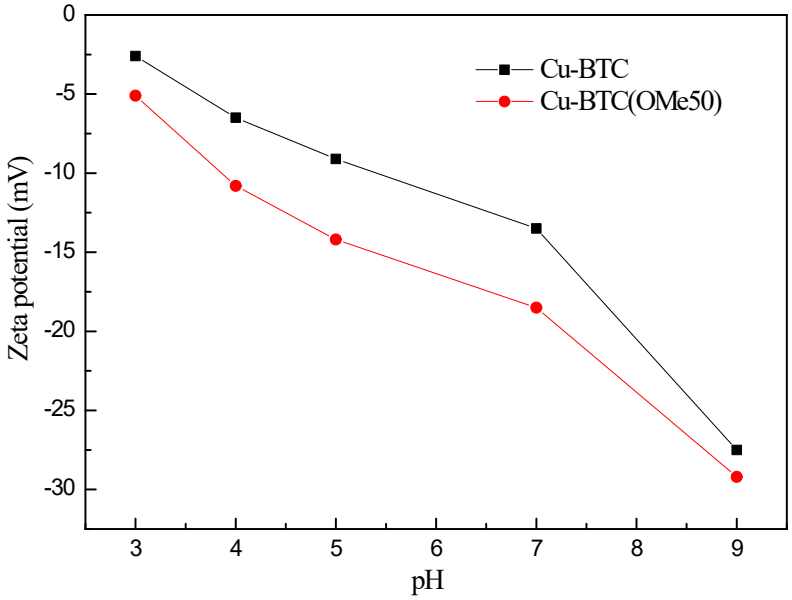

Fig. S6. Zeta potential of the Cu-BTC and Cu-BTC(OMe50).

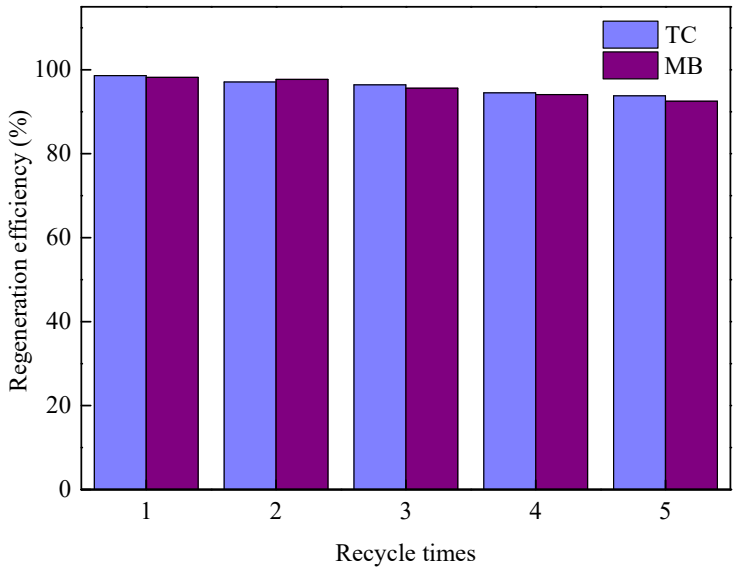

Fig. S7. Regenerated performances of Cu-BTC(OMe50) toward MB and TC.

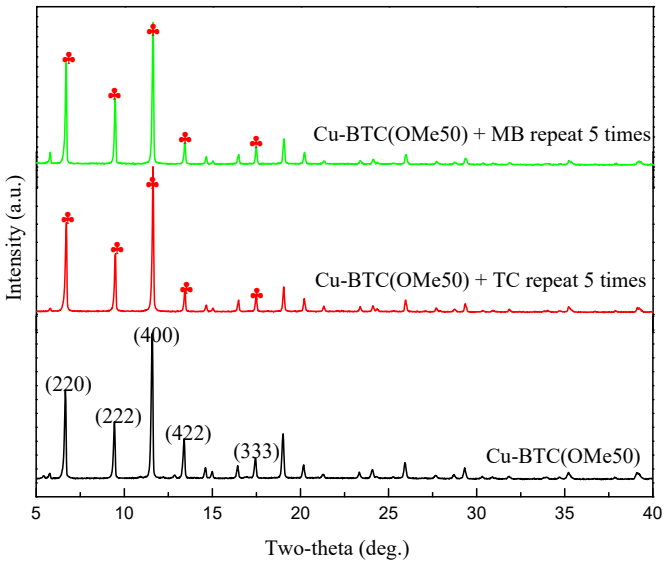

Fig. S8. XRD patterns of Cu-BTC(OMe50) repeated adsorption of MB and TC after fifth recycle.

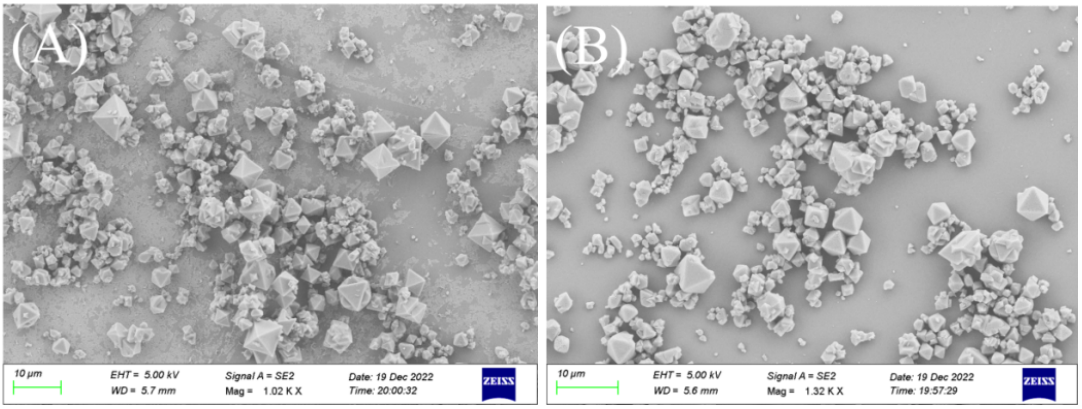

Fig. S9. SEM images of Cu-BTC(OMe50) repeated adsorption of MB(A) and TC(B) after fifth recycle.

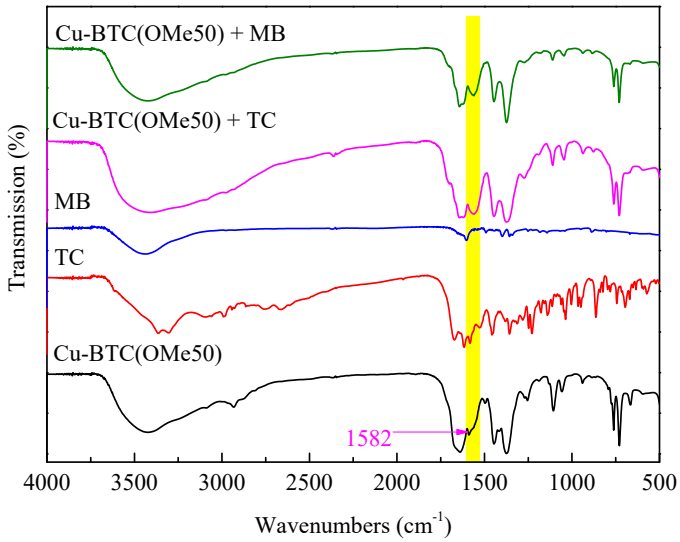

Fig. S10. FT-IR curves of Cu-BTC(OMe50) repeated adsorption of MB and TC after fifth recycle.

Table S1. Summary of textural properties of the samples

Samples	**S_{BET} ($m^2 \cdot g^{-1}$)**	**Pore volume ($cm^3 \cdot g^{-1}$)**	**Average pore size (nm)**
Cu-BTC	970	0.37	0.57
Cu-BTC(OMe50)	917	0.36	0.72
Cu-OMe	68	0.08	1.90

Table S2. Comparison of the MB and TC uptakes over some adsorbents

Adsorbates	Adsorbents	Uptake capacity (mg/g)	References
MB	Cu-BTC(OMe50)	138	This work
	M-Cu-BTC	0.3	[1]
	MIL-53(Al)	4	[2]
	HKUST-1/GO	14	[3]
	Fe_3O_4@ZIF-8	20	[4]
	Co/Fe-BDC	24	[5]
	JS-AC	60	[6]
	PEC/CS	170	[7]
	Pine leaves	123	[8]

Adsorbates	Adsorbents	Uptake capacity (mg/g)	References
	Ce-UiO-66	49	[9]
	MWCNTs	44	[10]
	γ-Fe_2O_3@P-graphene	125	[11]
	MMDM	7	[12]
TC	Cu-BTC(OMe50)	42	This work
	UiO-66(NH_2)	59	[13]
	NiCoFe-MOF-74	103	[14]
	In_2S_3/UiO-66	106	[15]
	MnUiO-66	72	[16]
	MSCG	32	[17]
	MGO	106	[18]
	Graphene oxide/Calcium alginate	132	[19]
	IMt-2	32	[20]
	HM	4.6	[21]
	HM-Fe	5.3	[21]
	MARG	24.2	[22]

References:

[1] A. R. Abbasi, M. Karimi, K. Daasbjerg, *Ultrason. Sonochem.*, 2017, **37**, 182-191.

[2] C. Li, Z. H. Xiong, J. M. Zhang, C. Wu, *J. Chem. Eng. Data*, 2015, **60**, 3414-3422.

[3] L. Li, X. L. Liu, H. Y. Geng, B. Hu, G.W. Song, Z.S. Xu, *J. Mater. Chem. A*., 2013, **1**, 10292.

[4] J. Zheng, C. Cheng, W.J. Fang, C. Chen, R.W. Yan, H.X. Huai, C.C. Wang, *Cryst. Eng. Comm.*, 2014, **16**, 3960-3964.

[5] S. Soni, P. K. Bajpai, J. Mittal, *J. Mol. Liq.*, 2020, **314**, 113642.

[6] R. Dod, G. Banerjee, D. R. Saini, *Clean Technol. Envir.*, 2015, **17**:,2349-2359.

[7] O. A. Attallah, W. Mamdouh, *Int. J. Environ. Sci. Te.*, 2021, **18**, 131-140.

[8] M. T. Yagub, T. K. Sen, H. M. Ang, *Water Air Soil Poll*., 2012, **223**, 5267-5282.

[9] M. R. Richelle, S. Ganesan, V. A. Kanalli, *J. Hazard. Mat*., 2021, **416**, 125941.

[10] D. L. Zhao, Y. Ding, S. H. Chen, *Asian J. Chem.*, 2013, **25**, 5756-5758.

[11] L. Y. Zhang, W. L. Zhang, Z. Q. Zhou, *J. Colloid Interf. Sci*., 2016, **476**, 200-205.

[12] H. John, G. Heba, M. Nour, *Sci. Total Environ*., 2020, **714**, 136832-136842.

[13] Y. Pan, X. Z. Yuan, L. B. Jiang, *Chem. Eng. J.,* 2020, **384**, 123310-123325.

[14] R. Xiao, H. I. Abdu, L. Wei, *Analyst*, 2020, **145**, 2398-2404.

[15] W. B. Dong, D. B. Wang, H. Wang, *J. Colloid Interf. Sci*., 2019, **535**, 444-457.

[16] Z. H. Yang, J. Cao, Y. P. Chen, *Micropor. Mesopor. Mat*., 2019, **277**, 277-285.

[17] B. Y. Huang, Y. G. Liu, B. Li, *Carbohyd. Polym*., 2017, **157**, 576-585.

[18] J. H. Miao, F. H. Wang, Y. J. Chen, *Appl. Surf. Sci*., 2019, **475**, 549-558.

[19] H. T. Zhu, T. Chen, J. Q. Liu, *RSC Adv.*, 2018, **8**, 2616-2621.

[20] P. H. Chang, Z. H. Li, J. S. Jean, W. T. Jiang, C. J. Wang, K. H. Lin, *Appl. Clay Sci.*, 2012, **67**, 158-163.

[21] H. B. Hou, G. L. Xu, F. He, H. Pan, *Int. J. Environ. Res*. 2023, **20**, 2901.

[22] D. Huang, J. Wu, L. Wang, X. Liu, J. Meng, X. Tang, *Chem. Eng. J.*, 2019, **358**, 1399-1409.

Table S3. Summary of fitting parameters of the adsorption isotherm model of MB by Cu-BTC and others.

Samples	Langmuir model			Freundlich model		
	$C_e/q_e=(1/q_{max})*C_e+1/(K_L*q_{max})$			$\ln q_e=\ln K_f+(1/n)*\ln C_e$		
	q_L (mg/g)	K_L (L/mg)	R^2	K_f (L/g)	n	R^2
Cu-BTC	20.04	0.0757	0.9498	3.2677	2.4931	0.6764
Cu-BTC(OMe50)	188.68	0.0941	0.9551	21.3681	1.7050	0.9005
Cu-OMe	61.35	0.0540	0.9249	6.9448	2.0691	0.7440

Table S4. Summary of fitting parameters of the adsorption isotherm model of TC by Cu-BTC and others.

Samples	Langmuir model			Freundlich model		
	$C_e/q_e=(1/q_{max})*C_e+1/(K_L*q_{max})$			$\ln q_e=\ln K_f+(1/n)*\ln C_e$		
	q_m (mg/g)	K_L (L/mg)	R^2	K_f (L/g)	n	R^2
Cu-BTC	32.26	0.0388	0.9472	2.9571	1.9999	0.8557
Cu-BTC(OMe50)	81.97	0.0172	0.9188	2.8095	1.4999	0.9263
Cu-OMe	81.97	0.0089	0.9101	1.2002	1.2933	0.9870

Table S5. Kinetics parameters on the adsorption of MB in solution by Cu-BTC and others.

Samples	Pseudo-first-order kinetic model						Pseudo-second-order kinetic model				
	$\ln(q_e-q_t)=\ln(q_{e\,cal})-k_1t$						$t/q_t=1/(K_2*q_e^2)+t/q_e$				
	$q_{e,exp}$ (mg/g)	$q_{e,cal}$ (mg/g)	K_1 (1/min)	R^2	$\triangle q$ (mg/g)	$\triangle q$ (%)	$q_{e,cal}$ (mg/g)	K_2 (g/mg·min)	R^2	$\triangle q$ (mg/g)	$\triangle q$ (%)
Cu-BTC	13.32	7.95	0.0104	0.9318	5.37	40.32	14.56	0.0019	0.9984	1.24	9.31
Cu-BTC(OMe50)	139.33	226.56	0.0123	0.9282	87.23	62.61	217.39	0.0000	0.9914	78.06	56.03
Cu-OMe	49.60	74.20	0.0124	0.9245	24.60	49.60	70.42	0.0000	0.9927	20.82	41.98

Table S6. Kinetics parameters on the adsorption of TC in solution by Cu-BTC and others.

Samples	Pseudo-first-order kinetic model						Pseudo-second-order kinetic model				
	$\ln(q_e-q_t)=\ln(q_{e\,cal})-k_1t$						$t/q_t=1/(K_2*q_e^2)+t/q_e$				
	$q_{e,exp}$ (mg/g)	$q_{e,cal}$ (mg/g)	K_1 (1/min)	R^2	$\triangle q$ (mg/g)	$\triangle q$ (%)	$q_{e,cal}$ (mg/g)	K_2 (g/mg·min)	R^2	$\triangle q$ (mg/g)	$\triangle q$ (%)
Cu-BTC	25.81	19.00	0.0290	0.9539	6.81	26.39	29.59	0.0016	0.9944	3.78	14.64
Cu-BTC(OMe50)	44.25	17.26	0.0198	0.9786	26.99	60.99	45.25	0.0031	0.9984	1.00	2.26
Cu-OMe	35.73	31.56	0.0374	0.9532	4.17	11.67	40.49	0.0014	0.9973	4.76	13.32